HHS Public Access

Author manuscript

Radiat Res. Author manuscript; available in PMC 2023 October 07.

Published in final edited form as:

Radiat Res. 2023 September 01; 200(3): 296–306. doi:10.1667/RADE-23-00052.1.

Impact of GADD45A on radiation biodosimetry using mouse peripheral blood

Constantinos G. Broustas[a,1], **Sanjay Mukherjee**[a], **Igor Shuryak**[a], **Alexandra Taraboletti**[b,c,2], **Jerry Angdisen**[b], **Pelagie Ake**[b], **Albert J. Fornace Jr.**[b,c], **Sally A. Amundson**[a]

[a]Center for Radiological Research, Columbia University Vagelos College of Physicians and Surgeons, Columbia University Irving Medical Center, New York, NY 10032, USA.

[b]Department of Oncology, Lombardi Comprehensive Cancer Center, Georgetown University Medical Center, Washington, DC 20057, USA.

[c]Department of Biochemistry and Molecular & Cellular Biology, Georgetown University Medical Center, Washington, DC 20057, USA.

Abstract

High-dose radiation exposure in a short period of time leads to - radiation syndromes characterized by severe acute and delayed organ-specific injury accompanied by elevated organismal morbidity and mortality. Radiation biodosimetry based on gene expression analysis of peripheral blood is a valuable tool to detect radiation exposure after a radiological/nuclear incident and obtain useful biological information that could predict tissue and organismal injury. However, confounding factors, including chronic inflammation, can potentially obscure the predictive power of the method. GADD45A (Growth arrest and DNA damage-inducible gene a) plays important roles in cell growth control, differentiation, DNA repair, and apoptosis. GADD45A-deficient mice develop an autoimmune disease, similar to human systemic lupus erythematosus, characterized by severe hematological disorders, kidney disease, and premature death. The goal of this study was to elucidate how pre-existing inflammation in mice, induced by *GADD45A* ablation, can affect radiation biodosimetry. We exposed wild-type and *GADD45A* knockout male C57BL/6J mice to 7 Gy X-rays and 24 h later RNA was isolated from whole blood and subjected to whole genome microarray and gene ontology analyses. Dose reconstruction analysis using a gene signature trained on gene expression data from irradiated wild-type male mice showed accurate reconstruction of 0 or 7 Gy doses with root mean square error of ± 1.05 Gy (R^2 = 1.00) in *GADD45A* knockout mice. Gene ontology analysis revealed that irradiation of both wild-type and *GADD45A*-null mice led to a significant overrepresentation of pathways associated with morbidity and mortality, as well as organismal cell death. However, based on their z-score, these pathways were predicted to be more significantly overrepresented in GADD45A-null mice, implying that *GADD45A* deletion may exacerbate the deleterious effects of radiation on blood cells. Numerous immune cell functions and quantities were predicted to be underrepresented in

[1]Correspondence should be addressed to: Dr. Constantinos G. Broustas, Center for Radiological Research, Columbia University Vagelos College of Physicians and Surgeons, 630 W. 168th St., New York, NY 10032; Tel.: 212-305-2187; cgb2117@cumc.columbia.edu.

[2]Current affiliation: Department of Chemistry, Division of Sciences and Mathematics, College of Arts and Sciences at the University of the District of Columbia, Washington, DC 20008, USA.

both genotypes; however, differentially expressed genes from irradiated *GADD45A* knockoutmice predicted an increased deterioration in the numbers of T lymphocytes, as well as myeloid cells, compared with wild-type mice. Furthermore, an overrepresentation of genes associated with radiation-induced hematological malignancies was associated with *GADD45A* knockoutmice, whereas hematopoietic and progenitor cell functions were predicted to be downregulated in irradiated *GADD45A* knockoutmice. In conclusion, despite the significant differences in gene expression between wild-type and GADD45A knockoutmice, it is still feasible to identify a panel of genes that could accurately distinguish between irradiated and control mice, irrespective of pre-existing inflammation status.

Keywords

GADD45A; radiation; biodosimetry; gene expression

INTRODUCTION

Accidental or intentional exposure of large numbers of individuals to high-dose ionizing radiation, such as in the case of a nuclear plant accident or the detonation of an improvised nuclear device, will result in organ specific sequelae of varying severity ranging from minimal effects that will need no medical attention to life-threating ones that will require appropriate therapeutic interventions. Radiation biodosimetry based on gene expression analysis of peripheral blood is a useful tool to reconstruct radiation dose exposure after a radiological/nuclear incident and obtain biological information that could predict the severity of organismal and tissue injury (1). However, confounding biological factors, including pre-existing medical conditions, such asautoimmune disease , could potentially obscure the predictive power of the method. It is estimated that autoimmune diseases are among the most prevalent diseases in the U.S. affecting more than 23.5 million people (2).

The GADD45 (Growth arrest and DNA damage) gene family consists of GADD45A, GADD45B, and GADD45G. These genes are often induced by DNA damage and other stress signals, and they have been implicated in the regulation of a wide variety of cellular processes, such as cell cycle arrest, DNA repair, apoptosis, genomic stability, chromatin remodeling, DNA demethylation, and innate and adaptive immunity (3-8). GADD45A is the only member of this family that is regulated by p53 (9) and contributes to the maintenance of genomic stability and cell growth control in response to genotoxic stress (10). Interestingly, the binding of p53 to the third intron of the *GADD45A* gene is necessary only in the case of ionizing radiation exposure and is not strictly required for the response to other insults such as UV radiation or the alkylating agent, methyl methanesulfonate (9). *GADD45A* knockout mice exhibit chromosomal abnormalities and increased radiation- and carcinogen-induced tumorigenesis (11-13), as well as delayed lung injury due to increased production of inflammatory cytokines in response to radiation (14).

GADD45A$^{-/-}$ mice develop and breed normally and do not show signs of disease until after 6 months of age (15). However, soon after, GADD45A-deficient mice spontaneously develop a lupus-like autoimmune disease that is characterized by the presence of

autoantibodies against double- and single-stranded DNA, as well as against histones (15), proteinuria and glomerulonephritis, reduced numbers of leukocytes and lymphocytes in their peripheral blood, followed by premature death predominantly in female mice (15). Similar sexual dimorphism of systemic lupus erythematosus incident is also observed in humans (16). These effects have been attributed to the hyperactivation of the alternative p38 mitogen-activated protein kinases (MAPK) signaling pathway in T lymphocytes (17). Specifically, following T-cell receptor-mediated activation, the non-receptor tyrosine kinase Zap70 phosphorylates and activates p38MAPK on Tyr323 in the absence of upstream mitogen activated protein kinase activation, whereas GADD45A inhibits this pathway and limits T cell hyperproliferation and autoimmunity. However, *GADD45A* null mice are hyper-responsive to activating stimuli due to spontaneously increased stress-activated p38 MAPK (17-19).

Within the innate immune system, GADD45 proteins contribute to the differentiation of myeloid cells. Absence of either GADD45A or GADD45b inhibited *in vitro* and *in vivo* differentiation of bone marrow cells into macrophages or granulocyte lineages and resulted in reduced frequencies and impaired the function of these cell types (20). In contrast, GADD45A or GADD45b deficiency resulted in higher proliferative capacity of immature myeloid cells (21). Steady-state myelopoiesis is not altered in *GADD45A*-null mice and no apparent abnormalities are observed in the number and types of hematopoietic cells in the bone marrow (21). However, *GADD45A*-null mice show impaired recovery of myeloid cells in the bone marrow after myeloablation using 5-fluorouracil treatment, and loss of either GADD45A or GADD45b impairs the response of myeloid cells to inflammatory stress.

In this study, we examined the impact of *GADD45A* knockout on peripheral mouse blood cell gene expression profiles 24 h following 7 Gy X-irradiation using male C57BL/6 mice and compared the data with wild-type mice treated under the same conditions. That particular time point was chosen as being relevant to early monitoring applications, and to allow direct comparison with our earlier studies, whereas whole blood was chosen as a minimally-invasive source for the development of molecular biomarkers. We applied a recently developed radiation dose reconstruction method (22) to determine the impact of GADD45A on this method of radiation biodosimetry. Furthermore, we performed gene ontology analysis to identify and compare differentially enriched pathways, diseases, and functions in wild-type and *GADD45A* knockout mice.

METHODS

Animals and irradiation

Wild-type C57BL/6 male mice were obtained from Charles River Laboratories (Frederick, MD) and generation of *GADD45A* knockout mice has been described previously (11). Animals were bred at Georgetown University with water and food ad libitum (12 h light / 12 h dark cycle conditions) according to Georgetown University Institutional Animal Care and Use Committee (GUACUC) protocols (2016-1152). Male mice that were 8 to 10 weeks old were exposed to a total body X-ray dose (0.86 Gy/min; X-Rad 320, Precision X-Ray Inc, Branford, CT; filter, 0.75 mm tin/ 0.25 mm copper/1.5 mm aluminum, 320 kV, 12.5 mA) of 0 or 7 Gy. The midline tissue (MLT) dose was measured with a RadCal ionization chamber

(10X6-6) connected to an Accu-Dose+ digitizer module with the chamber inserted inside the irradiation pie. Measurements were taken 3 times for 60 sec each and average dose rate was determined through the software Accu-Gold. Focus to skin distance (FSD) was 50cm with a 20x20 cm field size. Time of exposure was manually entered on the XRAD320. The mice were not anesthetized and were irradiated in a pie on a rotating table. Irradiations in the pie were conducted according to groups and genotypes, ranging between 5-9 mice at a time placed in a posterior-anterior (PA) position. Unirradiated animals were treated the same, with the exception that the machine was not turned on to irradiate the samples. Mice were divided into the following treatment groups: (1) unirradiated wild-type mice, (2), irradiated wild-type mice (3) unirradiated *GADD45A*$^{-/-}$ mice, (4) irradiated *GADD45A*$^{-/-}$ mice. Each group consisted of 5 mice, except for group 4 that consisted of 9 mice.

Blood Collection and RNA isolation

Blood was collected 1 day post-irradiation by cardiac puncture at the time of euthanasia (by CO_2 asphyxiation). Each sample (~0.4 ml blood) was added to a 15 ml centrifuge tube that contained 1.6 ml of PAXgene Blood RNA stabilization and lysis solution (PreAnalytix GmBH) and mixed thoroughly, while a small amount of blood was added to sodium EDTA anti-coagulant containing tubes for blood count using a Genesis hematology system (Oxford Science). After collection, blood was incubated at 4 °C for 24 h. RNA was purified following the PAXgene RNA kit recommendations with on-column DNase I treatment. As excessive amounts of globin transcript have been shown to interfere with gene expression signatures derived from blood, globin RNA was reduced using the Ambion GLOBINclear-mouse/rat kit (Thermofisher). RNA yields were quantified using the NanoDrop ND1000 spectrophotometer (Thermofisher) and RNA quality was checked by the 2100 Bioanalyzer (Agilent). High quality RNA with an RNA integrity number of at least 7.0 was used for microarray hybridization.

Microarray hybridization

Cyanine-3 labeled cRNA was prepared using the One-Color Low input Quick Amp Labeling kit (Agilent). Dye incorporation and cRNA yield was measured with a NanoDrop ND1000 spectrophotometer (Thermofisher). Labeled cRNA was fragmented and hybridized to Agilent Mouse Gene Expression 4x44K v2 Microarray Kit (G4846A). Slides were scanned with the Agilent DNA microarray scanner (G2505B) and the images were analyzed with Feature Extraction software (Agilent) using default parameters for background correction and flagging non-uniform features. The microarray data for the wild-type and GADD45A-null mice generated in this study have been deposited in the National Center for Biotechnology Information Gene Expression Omnibus (GEO) database with accession number GSE196400.

Data analysis

Background-corrected hybridization intensities were imported into BRB-ArrayTools, version 4.5.1 (23), $\log_2$-transformed and median normalized. Non-uniform outliers or features not significantly above background intensity in 25% or more of the hybridizations were filtered out. In addition, a minimum 1.5-fold change in at least 20% of the hybridizations was set as a requirement. Furthermore, probes were averaged to one probe

per gene and duplicate features were reduced by selecting the one with maximum signal intensity. The microarray data is available through the Gene Expression Omnibus with accession number GSE196400. Class comparison was conducted in BRB-ArrayTools to identify genes differentially expressed between radiation exposed samples and matched unirradiated controls using a random variance t-test. Genes with p-values less than 0.001 were considered statistically significant. The false discovery rate (FDR) was estimated for each gene by the method of Benjamini and Hochberg (24), to control for false positives. The cutoff in this analysis was set at an FDR of less than 0.05. Venn diagrams (25) were used to identify unique and overlapping differentially expressed genes from irradiated wild-type and *GADD45A* knockout mice.

Dose reconstruction

We analyzed two data sets of gene expression in mice: *GADD45* wild type (WT) and knockout . The WT data set was a priori assigned as a “training” data set for identifying radiation-responsive gene candidates, whereas the knockout data was assigned as a “testing” set where these candidate genes would be applied for dose reconstruction. The search for candidate genes in the “training” WT data was performed by selecting those genes which had a statistically significant positive or negative Pearson correlation coefficient with dose (either 0 or 7 Gy) and were measured (not missing) in all 10 samples. A p-value threshold of 0.05 with Bonferroni correction for multiple comparisons was selected to indicate statistical significance.

Top 10 candidate upregulated genes and top 10 downregulated genes from the WT "training" data set (i.e., genes with positive or negative statistically significant Pearson correlation coefficients with radiation dose) were selected for further analysis. Their signals were combined using geometric means, separately for upregulated and downregulated groups. The geometric means of top 10 upregulated and downregulated genes were calculated for both the WT and knockout data sets.

The net signal was defined as the difference in geometric means between upregulated and downregulated genes. A linear regression model was fitted the "training" WT data. The dependent (target) variable was radiation dose, and the independent (predictor) variable was the net signal of the genes. An intercept term was also allowed. The best-fit parameters for the regression model obtained on “training” data were then used to make dose predictions (reconstructions) on the "testing" data. Root mean squared errors (RMSE), mean absolute error (MAE) and coefficient of determination (R2) performance metrics, which compared actual with reconstructed dose values, were calculated to evaluate the model. These analyses were performed in R 4.2.0 software.

Gene ontology analysis

Lists of genes that were either significantly overexpressed or underexpressed compared with controls were analyzed using the Ingenuity Pathway Analysis (IPA) core pathway (Qiagen Ingenuity Systems) to identify significantly affected canonical pathways, diseases and functions. Benjamini corrected p values of < 0.05 were considered significant. Moreover,

the predicted activation state of each process was determined by its *z*-score. A z-score of at least 2 indicated activation, whereas a z-score of −2 or less indicated inactivation/inhibition.

RESULTS

Microarray analysis

Male mice were either sham-irradiated or exposed to 7 Gy of X-ray irradiation. Global gene expression was measured in the blood of mice sacrificed 1 day post-irradiation. Class comparison identified a total of 2,223 and 2,463 differentially expressed genes ($p < 0.001$, false discovery rate (FDR) < 5%) between unirradiated controls and irradiated wildtype or *GADD45A*-null peripheral blood, respectively (Fig. 1A and Supplementary File 1 for complete list of differentially expressed genes). Of the 4,686 differentially expressed genes in both genotypes, 1,061 (29.3%) genes were commonly responsive to radiation (Fig. 1B). However, their fold change differed markedly in the two genotypes (Fig. 1C). In general, absolute fold-changes, particularly among downregulated genes, were significantly lower for the *GADD45A* knockout mice than those of the wild-type mice in response to irradiation ($p = 1.54E-58$). Finally, only 85 genes were found to be differentially expressed in the two genotypes under basal (non-irradiated) conditions (Fig. 1A and Supplementary File 1).

Dose reconstruction

Next, we attempted a dose reconstruction analysis using the transcriptomic profile of wild-type animals as the training set. The initial search for genes significantly correlated with radiation dose in the “training” data identified 381 genes. The top 10 downregulated and top 10 upregulated genes from this group are shown in Table 1. Most of these genes showed similar dose-responsive trends in the “testing” data set (i.e., signs and magnitudes of Pearson correlation coefficients were similar to those in the “training” data), although they did not always reach statistical significance.

The best-fit parameters for a linear regression which predicted radiation dose on the “training” WT data were: intercept = 4.189 ± 0.040 (standard error); slope (dependence on gene net signal) = 0.962 ± 0.011, p-value = 3.07E-13. Using the net signal (difference) between geometric means of these 10 upregulated and downregulated genes allowed decently accurate dose reconstruction in the "testing" GADD45A knockout data set. For the 0 Gy group in the testing data, the mean reconstructed dose was 0.30 Gy with standard deviation of 1.64 Gy, and for the 7 Gy group in the testing data, the mean reconstructed dose was 6.91 Gy with standard deviation of 0.72 Gy. R^2 was 0.90, RMSE (Root Mean Square Error) was 1.05 Gy and MAE (Mean of Absolute value of Errors) was 0.85 Gy (Table 2).

Gene Ontology analysis

Of the 96 canonical pathways with a $|z| \geq 2.000$, 31 (32.3%) were significantly enriched in both wild-type and *GADD45A* knockout animals. Except for 3 pathways that were predicted to be activated based on their positive z-score values, the rest of the pathways were predicted to be inactivated in response to radiation (negative z-scores) (Supplementary File 2, tab 1). Among the common pathways, 10 pathways differed substantially ($|z| \geq 2.000$) in their z-scores denoting a differential impact of *GADD45A* on radiation-induced

gene expression compared with wild-type mice. Half of these canonical pathways were related to phosphoinositide metabolism (Supplementary File 2, tab 1). In contrast, only 3 (3.1%) canonical pathways were significant in wild-type irradiated mice alone, whereas 62 pathways (64.6%) were predicted to be significant only in the knockout mice. The majority of canonical pathways that were predicted to be underrepresented in the GADD45A knockout mice were related to signaling pathways, such as “NGF Signaling” ($z = -4.243$), “HGF Signaling” ($z = -3.536$), “GM-CSF Signaling” ($z = -3.130$), and “PDGF Signaling” ($z = -2.600$). Furthermore, DNA damage and repair pathways, such as “Nucleotide Excision Repair Pathway” ($z = -3.413$) and “Salvage Pathways of Pyrimidine Ribonucleotides” ($z = 3.024$) (26) were underrepresented exclusively in the GADD45A knockout mice.

Further analysis revealed that 239 diseases and functions were predicted to be differentially regulated in irradiated mice compared with unirradiated mice. Of these, 46 (19.5%) functions were common to both genotypes, whereas 18 (7.5%) and 175 (73.2%) were uniquely enriched in wild-type and *GADD45A* knockout mice, respectively. Among the functions shared by both genotypes, 20 (43.4%) had significantly ($|z| \geq 2.000$) different z-scores in *GADD45A* knockout vs. wild-type mice, whereas the opposite was never predicted (Supplementary File 2, tab 2).

Differentially expressed genes in irradiated *vs.* unirradiated wild-type mice were enriched in functions such as “Organismal death” ($z = 4.194$) and “Morbidity and mortality” ($z = 4.284$). Concordantly, cell viability ($z = -2.701$) and survival ($z = -2.889$), as well as quantities of various cell types were underrepresented, whereas cell death-related pathways were overrepresented (Fig. 2A shows top-20 functions and Supplementary File 2, tab 2 contains the complete list of significant functions). Irradiated GADD45A-null mice differentially represented the same functions, albeit with significantly different z-scores. Thus, “Organismal death” ($z = 14.569$), “Morbidity and mortality” ($z = 14.519$) were overrepresented, whereas “cell viability/survival” ($z = -5.062/-5.196$) were underrepresented. In addition, “growth failure or short stature” ($z = 7.771$) and “hypoplasia” ($z = 7.364$), especially of lymphatic system ($z = 7.465$), were enriched exclusively in *GADD45A* knockoutirradiated mice. Moreover, quantities of various immune cell-related functions, particularly those related to T lymphocytes and myeloid cells, were underrepresented with absolute z-scores significantly higher than wild-type mice (Fig. 2A and Supplementary File 2, tab 2). In addition, B lymphocyte, and quantities of IgGs were underrepresented in both wild type and *GADD45A*-null mice with similar z-scores. Moreover, a number of functions related to myeloid cell activation and migration, such as “Chemotaxis of myeloid cells” ($z = -2.058$), “Recruitment of myeloid cells” ($z = -2.128$), and “Migration of myeloid cells” ($z = -2.262$), “Cell movement of myeloid cells” ($z = -2.932$), were specifically underrepresented in the GADD45A knockout blood following irradiation (Fig. 2B).

Consistent with previous reports (27), phagocytosis-related functions defined by terms “phagocytosis”, “engulfment”, and “endocytosis” were enriched in irradiated wild-type blood cells (Fig. 2C). For example, “Engulfment of cells” ($z = 2.850$), “Phagocytosis of cells” ($z = 2.618$), and “Endocytosis by eukaryotic cells” ($z = 2.237$) were uniquely

overrepresented in wild-type mice. In contrast, none of these functions were overrepresented in irradiated knockout mice (Fig. 2C).

A special class of biofunctions related to hematopoietic stem and progenitor cell functions and development and differentiation of the hematopoietic system, such as “Differentiation of hematopoietic progenitor cells” (z = −2.242) and “Development of hematopoietic progenitor cells” (z = −3.528) were underrepresented in the GADD45A knockout mice after X-irradiation. In contrast, no enrichment of hematopoietic stem cell-related functions was significant in irradiated wild-type animals (Fig. 2D).

GADD45 is induced by DNA damage and other stress signals and many of these roles are carried out via signaling mediated by p38 mitogen-activated protein kinases (MAPKs) (3). We compared the gene expression profiles of wild-type and GADD45A knockout irradiated mice with our previous transcriptomic data derived from p38MAPK dominant negative (DN: $p38\alpha^{AF/+}$) (28) and double knockin (DKI: $p38\alpha\beta^{Y323F}$) (29) mice that had been exposed to the same radiation dose and dose rate and examined 24 h post-irradiation (30). We showed that p38MAPK downregulation was associated with overrepresentation of pro-survival immune cell functions (Fig. 3A and Supplementary Table 1 for the complete list of significant cell survival- and death-related biofunctions), as well as phagocytosis-associated functions (Fig. 3B) compared with wild-type animals. In contrast, in irradiated *GADD45A*-nullperipheral blood cells these functions were opposite (negative z-score) to p38MAPK mutant mice (Fig. 3A and B and Supplementary Table 1).

Finally, among the differentially regulated functions in irradiated *GADD45A*-nullmice that were overrepresented were numerous cancer-related diseases, specifically hematological cancers or lymphoproliferative disorders with a concomitant increase in cell death (Fig. 4). Both lymphoid and myeloid-related cancers were enriched in the irradiated *GADD45* knockout mouse peripheral blood. In contrast, none of these functions were significantly represented in irradiated wild-type mice.

DISCUSSION

A prerequisite for the successful management of radiation sequelae, especially in situations, , that involve large numbers of people who may or may not have been exposed to potentially harmful doses, is to use a biodosimetry technique to assess radiation dose exposure, as a surrogate of radiation injury. Large-scale transcriptomic analysis using whole blood has been used to select genes that may detect radiation exposure both in humans and mice (27, 31-38). However, blood-based gene expression signatures should be tested against various potential confounding variables, including age, sex, or inflammation. In our previous works we focused on the impact of age, sex, DNA repair defects, and differential inflammatory status. We showed that age could have a profound impact on gene expression and diminish the predictive power of a radiation biodosimetry gene list previously created using young animals as the training set (27), especially in aged female mice *vs.* aged male mice (36). These results suggested that identification of radiation biomarker candidates should be robust enough to translate across age or sex. In contrast, using two transgenic mouse models that mimic chronic inflammation (*IL-10* knockout)

(39) and anti-inflammation, such as in the case of anti-inflammatory or immunosuppressive medication, recreated in mice using the double knockin *p38αβ*^{MAPK} and the dominant negative *p38α*^{MAPK} transgenes (30), showed that despite the widespread transcriptomic changes in radiation-exposed mice of different genotypes, it was still possible to accurately reconstruct radiation dose. In our current study, we focused on the stress-responsive gene *GADD45A* that has pleiotropic effects on both the adaptive and the innate branches of the immune system, as well as on hematopoietic stem and progenitor cells that are necessary to reconstitute the immune system after a high-dose radiation assault. We elucidated the impact of GADD45A deletion on the accuracy of a gene expression signature derived from irradiated wild-type mouse peripheral blood cells and tested it on the *GADD45A* knockout dataset to reconstruct the actual radiation dose, using a dose reconstruction algorithm developed in our lab (22). Using this method, we were able to define a gene expression signature that could reconstruct the radiation dose of 0 or 7 Gy with root mean square error of ± 1.05 Gy with a coefficient of determination (R^2) of 1.00. These data showed that *GADD45A* deletion does not limit the robustness of the reconstructed dose estimate. However, deletion of *GADD45A* had a profound effect on several pathways and functions that could affect the severity of injury.

Cell death and specifically apoptosis plays multiple critical roles in the immune system, such as the negative selection of thymocytes and lymphocytes, as a defense mechanism against autoimmunity, and in the maintenance of proliferative homeostasis (40). Furthermore, it is well known that proliferating hematopoietic system cells predominantly undergo apoptosis in response to irradiation (41). Our analysis showed that the gene expression profile in peripheral blood cells from wild-type mice exposed to radiation correlated with an enrichment of cell death-related functions, whereas functions associated with quantity of many immune cell subtypes were markedly underrepresented. However, *GADD45A*-null were predicted to be significantly more sensitive to radiation since they showed enrichment of organismal death and morbidity or mortality with a concomitant decrease in cell viability with z-scores that are far greater than those of wild-type mice. Our previous transcriptomic analysis of irradiated mice (30) predicted that p38MAPK signaling impairment will protect mice from organismal and cell death following radiation exposure, whereas here we found the implication that *GADD45A* ablation greatly exacerbates organismal and cell death in irradiated mice, thus implying a protective role of GADD45A in DNA damage-induced hematopoietic injury by opposing both the classical and the alternative p38MAPK signaling pathway activation. Furthermore, our bioinformatic analysis revealed that T lymphocyte-related functions were underrepresented mostly in the *GADD45A* knockout mice exposed to radiation, whereas functions associated with quantities of B lymphocytes were affected in common, with both wild-type and *GADD45A* knockout mice showing comparable z-scores. This observation is in agreement with the well-established role of GADD45A as a negative regulator of p38MAPK signaling during T cell activation and subsequent proliferation by inhibiting the p38MAPK alternative pathway (19), whereas *GADD45A* ablation causes abnormal p38MAPK phosphorylation and activation, T cell hyperproliferation, and lupus-like autoimmune disease in mice (15, 17). Thus, it appears that GADD45A may have a negative impact on p38MAPK activation not only in response to T cell receptor activation, but also after genotoxic stress.

Phagocytosis is predominantly carried out by the so-called professional phagocytes that belong to the myeloid cell lineage, including macrophages, dendritic cells, and neutrophils and it is crucial in maintaining tissue homeostasis and innate immune balance and it is tasked with the clearance of apoptotic cells, as well as invading pathogens such as bacteria and microbes (42). Dysfunctional phagocytosis leads to accumulation of unphagocytosed debris with subsequent accumulation of secondary necrotic debris that promotes chronic inflammation and autoimmune diseases (43), such as systemic lupus erythematosus 44-46,), and exacerbates tissue damage. We have shown previously that phagocytosis-related functions are enriched in irradiated young mice, but not aged mice (27). Furthermore, ablation of the p38MAPK signaling pathway in mice exposed to radiation showed a greater enrichment in phagocytosis functions, implying that p38MAPK may act as an inhibitor of the process (30). In the current analysis, we confirmed that phagocytosis functions were significantly overrepresented in wild-type mice following high dose radiation. However, phagocytosis-related functions were underrepresented in *GADD45A* knockout mice. We postulate that GADD45A ablation results in elevated p38MAPK signaling activity following radiation exposure, which, in turn, would lead to diminished phagocytosis activity and promote a pro-inflammatory phenotype, known to be observed in *GADD45A*-null mice. Finally, under basal conditions, phagocytosis-related functions were not significantly enriched in either genotype.

Evidence exists that implicates GADD45A in myeloid innate immune functions, including reactive oxygen species production, phagocytosis, and adhesion (20). Although no apparent abnormalities are observed in either the bone marrow or peripheral blood compartments of mice deficient for *GADD45A* (47), under hematological stress, including acute stimulation with cytokines, myeloablation, and inflammation, *GADD45A*-null (or *GADD45b*-null) mice exhibit reduced bone marrow cellularity, poor recovery of the mature myeloid compartment compared to wild type controls (21, 47-49), and impaired terminal differentiation and survival of myeloid cells in response to acute stimulation with cytokines (21). Furthermore, myeloid-enriched bone marrow cells from *GADD45A* (and *GADD45b*) deficient mice are more sensitive to genotoxic stress (48), implying that GADD45A has pro-survival functions in these cells. In line with these findings, our study predicts *GADD45A* ablation has a negative impact on the myeloid cell compartment after irradiation with markedly underrepresented myeloid cell survival and differentiation functions.

Hematopoietic stem and progenitor cells maintain blood cell homeostasis through their ability of self-renewal and differentiation into functionally mature blood cell subtypes. Their ability to reconstitute the immune system following genotoxic insults is crucial for the survival and recovery of the organism. GADD45A is upregulated in hematopoietic stem cells in response to ionizing radiation, but its exact role remains controversial (50, 51). It has been reported that GADD45A loss enhances hematopoietic stem cell reconstitution after hematopoietic stress (50). Conversely, it has also been reported that GADD45A upregulation accelerates hematopoietic stem cell differentiation (51). Our gene expression analysis is in line with the conclusions of Wingert et al (51), since they suggest that GADD45A may have a negative impact on hematopoietic and progenitor cell survival, proliferation, and differentiation, as these functions were significantly underrepresented, whereas the same functions were not predicted to be statistically enriched by radiation in wild-type animals.

Aberrant GADD45A protein expression has been associated with numerous human malignancies and GADD45A oncogenic stress functions depend on the cell type, developmental stage, and nature of stress/stimulus (3, 52, 53). Our bioinformatic analysis revealed that radiation exposure of *GADD45A*-null mice, but not wild-type, was associated with an overrepresentation of functions related to various malignancies, predominantly blood cancers. Previous reports have also demonstrated that *GADD45*-null mice display increased susceptibility to radiation-induced carcinogenesis and the cause of death has been attributed to increased incident of lymphomas (11). Specifically, long-term survival studies have indicated that *GADD45*$^{-/-}$ mice exposed to fractionated radiation succumb to death at increased rates compared to wild-type irradiated mice, whereas GADD45A$^{+/-}$ have an intermediate death rate (11). In other malignancies, inactivation of GADD45A sensitizes epithelial cancer cells to ionizing radiation resulting in prolonged survival (54), whereas radiation-induced human GADD45 expression correlates with clinical response to radiotherapy of cervical carcinoma (55). Thus, GADD45A acts as a tumor suppressor in radiation-induced hematological and solid malignancies.

In conclusion, our data show that *GADD45A* ablation did not have a significant influence on radiation dose estimates, at least at 7 Gy X-rays. However, further studies using a range of radiation doses, both high and low, will be necessary to fully understand the impact of GADD45A on gene expression-based radiation biodosimetry. Previously, we investigated the impact of dose rates that would be directly relevant to a large-scale event, such as low-dose rate and internal emitter effects relevant to fallout or a radiological dispersal device (56-61). Future studies will also use the ultra-high dose rate irradiator we have developed (62) to deliver doses on a micro-second scale, relevant to the prompt radiation emitted by an improvised nuclear device. In this work we have used mice of only one sex (male) to show proof of principle. However, emerging evidence suggests that radiosensitivity differs between males and females in various animal models (63, 64). Furthermore, recently, we have demonstrated that sex differences affect gene expression signatures in response to radiation exposure (36). Thus, it will be important to compare the results of the current study in both sexes in future studies. Gene ontology analysis demonstrated that there are significant variations of enriched biological pathways, diseases, and functions among wild-type and *GADD45A*-null animals, which suggest that GADD45A may have an impact on the susceptibility to and severity of radiation injury. Although our transcriptomic analysis reveals that *GADD45A* knockout is predicted to reduce animal survival in response to a single high-dose total body X-irradiation, formal animal survival assays will be necessary to definitely prove this effect. Furthermore, gene ontology analysis of the differentially expressed genes could help identify important biological functions that could be used to rationally design new radio-mitigators. However, to validate the findings of the present study, functional studies will be necessary to causally connect the differentially enriched pathways with the severity of radiation damage.

Supplementary Material

Refer to Web version on PubMed Central for supplementary material.

ACKNOWLEGMENTS

Analyses were performed using the BRB-ArrayTools developed by Dr. Richard Simon and the BRB-ArrayTools Development Team. We would like to thank Dr. Evagelia Laiakis for advice with the mouse irradiation conditions. This work was supported by the Center for High-Throughput Minimally-Invasive Radiation Biodosimetry, National Institute of Allergy and Infectious Diseases Grant number U19AI067773.

ABBREVIATIONS

FDR	False Discovery Rate
IPA	Ingenuity Pathway Analysis
WT	wild-type
KO	GADD45A knockout
ir	irradiated
ui	unirradiated

REFERENCES

1. Sproull M, Camphausen K. State-of-the-art advances in radiation biodosimetry for mass casualty events involving radiation exposure. Radiat Res. 2016; 186:423–435. [PubMed: 27710702]
2. National Institutes of Health Autoimmune Disease Coordinating Committee Report. 2002. Bethesda (MD): The Institutes; 2002.
3. Humayun A, Fornace AJ Jr. GADD45 in stress signaling, cell cycle control, and apoptosis. Adv Exp Med Biol. 2022; 1360:1–22. [PubMed: 35505159]
4. Chandramouly G GADD45 in DNA demethylation and DNA repair. Adv Exp Med Biol. 2022; 1360:55–67. [PubMed: 35505162]
5. Gao M, Guo N, Huang C, Song L. Diverse roles of GADD45Alpha in stress signaling. Curr Protein Pept Sci. 2009; 10:388–94. [PubMed: 19689359]
6. Ma DK, Guo JU, Ming GL, Song H. DNA excision repair proteins and GADD45 as molecular players for active DNA demethylation. Cell Cycle. 2009; 8:1526–31. [PubMed: 19377292]
7. Tran H, Brunet A, Grenier JM, Datta SR, Fornace AJ Jr, DiStefano PS, et al. DNA repair pathway stimulated by the forkhead transcription factor FOXO3a through the GADD45 protein. Science. 2002; 296:530–4. [PubMed: 11964479]
8. Carrier F, Georgel PT, Pourquier P, Blake M, Kontny HU, Antinore MJ, et al. GADD45, a p53-responsive stress protein, modifies DNA accessibility on damaged chromatin. Mol Cell Biol. 1999; 19:1673–85. [PubMed: 10022855]
9. Kastan MB, Zhan Q, el-Deiry WS, Carrier F, Jacks T, Walsh WV, et al. A mammalian cell cycle checkpoint pathway utilizing p53 and GADD45 is defective in ataxia-telangiectasia. Cell. 1992; 71:587–97. [PubMed: 1423616]
10. Hollander MC, Fornace AJ Jr. Genomic instability, centrosome amplification, cell cycle checkpoints and GADD45A. Oncogene. 2002; 21:6228–33. [PubMed: 12214253]
11. Hollander MC, Sheikh MS, Bulavin DV, Lundgren K, Augeri-Henmueller L, Shehee R, et al. Genomic instability in GADD45A-deficient mice. Nat Genet. 1999; 23:176–84. [PubMed: 10508513]
12. Hollander MC, Kovalsky O, Salvador JM, Kim KE, Patterson AD, Haines DC, et al. Dimethylbenzanthracene carcinogenesis in GADD45A-null mice is associated with decreased DNA repair and increased mutation frequency. Cancer Res. 2001; 61:2487–91. [PubMed: 11289119]

13. Hildesheim J, Bulavin DV, Anver MR, Alvord WG, Hollander MC, Vardanian L, et al. GADD45A protects against UV irradiation-induced skin tumors, and promotes apoptosis and stress signaling via MAPK and p53. Cancer Res. 2002; 62:7305–15. [PubMed: 12499274]
14. Mathew B, Takekoshi D, Sammani S, Epshtein Y, Sharma R, Smith BD, et al. Role of GADD45A in murine models of radiation- and bleomycin-induced lung injury. Am J Physiol Lung Cell Mol Physiol. 2015; 309:L1420–9. [PubMed: 26498248]
15. Salvador JM, Hollander MC, Nguyen AT, Kopp JB, Barisoni L, Moore JK, et al. Mice lacking the p53-effector gene GADD45A develop a lupus-like syndrome. Immunity. 2002; 16:499–508. [PubMed: 11970874]
16. Tsokos GC. Systemic lupus erythematosus. N Engl J Med. 2011; 365(22):2110–21. [PubMed: 22129255]
17. Salvador JM, Mittelstadt PR, Belova GI, Fornace AJ Jr, Ashwell JD. The autoimmune suppressor GADD45Alpha inhibits the T cell alternative p38 activation pathway. Nat Immunol. 2005; 6:396–402. [PubMed: 15735649]
18. Salvador JM, Mittelstadt PR, Guszczynski T, Copeland TD, Yamaguchi H, Appella E, et al. Alternative p38 activation pathway mediated by T cell receptor-proximal tyrosine kinases. Nat Immunol. 2005; 6:390–5. [PubMed: 15735648]
19. Ashwell JD. The many paths to p38 mitogen-activated protein kinase activation in the immune system. Nat Rev Immunol. 2006; 6:532–40. [PubMed: 16799472]
20. Salerno DM, Tront JS, Hoffman B, Liebermann DA. GADD45A and GADD45b modulate innate immune functions of granulocytes and macrophages by differential regulation of p38 and JNK signaling. J Cell Physiol. 2012; 227:3613–20. [PubMed: 22307729]
21. Gupta SK, Gupta M, Hoffman B, Liebermann DA. Hematopoietic cells from GADD45A-deficient and GADD45b-deficient mice exhibit impaired stress responses to acute stimulation with cytokines, myeloablation and inflammation. Oncogene. 2006; 25:5537–46. [PubMed: 16732331]
22. Ghandhi SA, Smilenov L, Shuryak I, Pujol-Canadell M, Amundson SA. Discordant gene responses to radiation in humans and mice and the role of hematopoietically humanized mice in the search for radiation biomarkers. Sci Rep. 2019; 9:19434. [PubMed: 31857640]
23. Wright GW, Simon RM. A random variance model for detection of differential gene expression in small microarray experiments. Bioinformatics. 2013; 19:2448–55.
24. Hochberg Y, Benjamini Y. More powerful procedures for multiple significance testing. Stat Med. 1990; 9:811–8. [PubMed: 2218183]
25. Oliveros JC (2007-2015) Venny. An interactive tool for comparing lists with Venn's diagrams. https://bioinfogp.cnb.csic.es/tools/venny/index.html
26. Austin WR, Armijo AL, Campbell DO, Singh AS, Hsieh T, Nathanson D, et al. Nucleoside salvage pathway kinases regulate hematopoiesis by linking nucleotide metabolism with replication stress. J Exp Med. 2012; 209:2215–28. [PubMed: 23148236]
27. Broustas CG, Duval AJ, Amundson SA. Impact of aging on gene expression response to x-ray irradiation using mouse blood. Sci Rep. 2021; 11:10177. [PubMed: 33986387]
28. Wong ES, Le Guezennec X, Demidov ON, Marshall NT, Wang ST, Krishnamurthy J, et al. p38MAPK controls expression of multiple cell cycle inhibitors and islet proliferation with advancing age. Dev Cell. 2009; 17:142–9. [PubMed: 19619499]
29. Jirmanova L, Giardino Torchia ML, Sarma ND, Mittelstadt PR, Ashwell JD. Lack of the T cell-specific alternative p38 activation pathway reduces autoimmunity and inflammation. Blood. 2011; 118:3280–9. [PubMed: 21715315]
30. Broustas CG, Mukherjee S, Pannkuk EL, Laiakis EC, Fornace AJ, Amundson SA. Effect of the p38 Mitogen-activated protein kinase signaling cascade on radiation biodosimetry. Radiat Res. 2022; 198:18–27. [PubMed: 35353886]
31. Dressman HK, Muramoto GG, Chao NJ, Meadows S, Marshall D, Ginsburg GS, et al. Gene expression signatures that predict radiation exposure in mice and humans. PLoS Med. 2007; 4:e106. [PubMed: 17407386]
32. Paul S, Amundson SA. Gene expression signatures of radiation exposure in peripheral white blood cells of smokers and non-smokers. Int J Radiat Biol. 2011; 87:791–801. [PubMed: 21801107]

33. Broustas CG, Xu Y, Harken AD, Chowdhury M, Garty G, Amundson SA. Impact of neutron exposure on global gene expression in a human peripheral blood model. Radiat Res. 2017; 187:433–440.
34. Broustas CG, Xu Y, Harken AD, Garty G, Amundson SA. Comparison of gene expression response to neutron and x-ray irradiation using mouse blood. BMC Genomics. 2017; 18:2. [PubMed: 28049433]
35. Broustas CG, Harken AD, Garty G, Amundson SA. Identification of differentially expressed genes and pathways in mice exposed to mixed field neutron/photon radiation. BMC Genomics. 2018; 19:504. [PubMed: 29954325]
36. Broustas CG, Shuryak I, Duval AJ, Amundson SA. Effect of age and sex on gene expression-based radiation biodosimetry using mouse peripheral blood. Cytogenet Genome Res. 2023; doi: 10.1159/000530172.
37. Mukherjee S, Grilj V, Broustas CG, Ghandhi SA, Harken AD, Garty G, et al. Human transcriptomic response to mixed neutron-photon exposures relevant to an improvised nuclear device. Radiat Res. 2019; 192:189–199. [PubMed: 31237816]
38. Li S, Lu X, Feng JB, Tian M, Wang J, Chen H, et al. Developing gender-specific gene expression biodosimetry using a panel of radiation-responsive genes for determining radiation dose in human peripheral blood. Radiat Res. 2019; 192:399–409. [PubMed: 31373872]
39. Mukherjee S, Laiakis EC, Fornace AJ Jr, Amundson SA. Impact of inflammatory signaling on radiation biodosimetry: mouse model of inflammatory bowel disease. BMC Genomics. 2019; 20:329. [PubMed: 31046668]
40. Salminen A, Ojala J, Kaarniranta K. Apoptosis and aging: increased resistance to apoptosis enhances the aging process. Cell Mol Life Sci. 2011; 68:1021–31. [PubMed: 21116678]
41. Sarosiek KA, Fraser C, Muthalagu N, Bhola PD, Chang W, McBrayer SK, et al. Developmental regulation of mitochondrial apoptosis by c-Myc governs age- and tissue-specific sensitivity to cancer therapeutics. Cancer Cell. 2017; 31:142–156. [PubMed: 28017613]
42. Li W. Phagocyte dysfunction, tissue aging and degeneration. Ageing Res Rev. 2013; 12:1005–12. [PubMed: 23748186]
43. A-Gonzalez N, Bensinger SJ, Hong C, Beceiro S, Bradley MN, Zelcer N, et al. Apoptotic cells promote their own clearance and immune tolerance through activation of the nuclear receptor LXR. Immunity. 2009; 31:245–58. [PubMed: 19646905]
44. Herrmann M, Voll RE, Zoller OM, Hagenhofer M, Ponner BB, Kalden JR. Impaired phagocytosis of apoptotic cell material by monocyte-derived macrophages from patients with systemic lupus erythematosus. Arthritis Rheum. 1998; 41:1241–50. [PubMed: 9663482]
45. Gaipl US, Voll RE, Sheriff A, Franz S, Kalden JR, Herrmann M. Impaired clearance of dying cells in systemic lupus erythematosus. Autoimmun Rev. 2005; 4:189–94. [PubMed: 15893710]
46. Savill J. Apoptosis in resolution of inflammation. J Leukoc Biol. 1997; 61:375–80. [PubMed: 9103222]
47. Liebermann DA. GADD45 in normal hematopoiesis and leukemia. Adv Exp Med Biol. 2022; 1360:41–54. [PubMed: 35505161]
48. Gupta M, Gupta SK, Balliet AG, Hollander MC, Fornace AJ, Hoffman B, et al. Hematopoietic cells from GADD45A- and GADD45b-deficient mice are sensitized to genotoxic-stress-induced apoptosis. Oncogene. 2005; 24:7170–9. [PubMed: 16170381]
49. Hoffman B, Liebermann DA. GADD45 modulation of intrinsic and extrinsic stress responses in myeloid cells. J Cell Physiol. 2009; 218:26–31. [PubMed: 18780287]
50. Chen Y, Ma X, Zhang M, Wang X, Wang C, Wang H, et al. GADD45A regulates hematopoietic stem cell stress responses in mice. Blood. 2014; 123:851–62. [PubMed: 24371210]
51. Wingert S, Thalheimer FB, Haetscher N, Rehage M, Schroeder T, Rieger MA. DNA-damage response gene GADD45A induces differentiation in hematopoietic stem cells without inhibiting cell cycle or survival. Stem Cells. 2016; 34:699–710. [PubMed: 26731607]
52. Tront JS, Hoffman B, Liebermann DA. GADD45A suppresses Ras-driven mammary tumorigenesis by activation of c-Jun NH2-terminal kinase and p38 stress signaling resulting in apoptosis and senescence. Cancer Res. 2006; 66:8448–54. Erratum in: Cancer Res. 2007; 67:427. [PubMed: 16951155]

53. Alam MS, Gaida MM, Bergmann F, Lasitschka F, Giese T, Giese NA, et al. Selective inhibition of the p38 alternative activation pathway in infiltrating T cells inhibits pancreatic cancer progression. Nat Med. 2015; 21:1337–43. [PubMed: 26479921]
54. Lu X, Yang C, Hill R, Yin C, Hollander MC, Fornace AJ Jr, et al. Inactivation of GADD45A sensitizes epithelial cancer cells to ionizing radiation in vivo resulting in prolonged survival. Cancer Res. 2008; 68:3579–83. [PubMed: 18483238]
55. Santucci MA, Barbieri E, Frezza G, Perrone A, Iacurti E, Galuppi A, et al. Radiation-induced GADD45 expression correlates with clinical response to radiotherapy of cervical carcinoma. Int J Radiat Oncol Biol Phys. 2000; 46:411–6. [PubMed: 10661348]
56. Paul S, Smilenov LB, Elliston CD, Amundson SA. Radiation Dose-Rate Effects on Gene Expression in a Mouse Biodosimetry Model. Radiat Res. 2015;184:24–32. [PubMed: 26114327]
57. Ghandhi SA, Smilenov LB, Elliston CD, Chowdhury M, Amundson SA. Radiation dose-rate effects on gene expression for human biodosimetry. BMC Med Genomics. 2015;8:22. [PubMed: 25963628]
58. Abend M, Amundson SA, Badie C, Brzoska K, Hargitai R, Kriehuber R, et al. Inter-laboratory comparison of gene expression biodosimetry for protracted radiation exposures as part of the RENEB and EURADOS WG10 2019 exercise. Sci Rep. 2021;11:9756. [PubMed: 33963206]
59. Paul S, Ghandhi SA, Weber W, Doyle-Eisele M, Melo D, Guilmette R, et al. Gene expression response of mice after a single dose of 137CS as an internal emitter. Radiat Res. 2014;182:380–9. [PubMed: 25162453]
60. Ghandhi SA, Weber W, Melo D, Doyle-Eisele M, Chowdhury M, Guilmette R, et el. Effect of 90Sr internal emitter on gene expression in mouse blood. BMC Genomics. 2015;16:586. [PubMed: 26251171]
61. Ghandhi SA, Sima C, Weber WM, Melo DR, Rudqvist N, Morton SR, et al. Dose and Dose-Rate Effects in a Mouse Model of Internal Exposure to 137Cs. Part 1: Global Transcriptomic Responses in Blood. Radiat Res. 2020;196:478–490. [PubMed: 32931585]
62. Garty G, Obaid R, Deoli N, Royba E, Tan Y, Harken AD, et al. Ultra-high dose rate FLASH irradiator at the radiological research accelerator facility. Sci Rep. 2022;12:22149. [PubMed: 36550150]
63. Beach T, Authier S, Javitz HS, Wong K, Bakke J, Gahagen J, et al. Total body irradiation models in NHPs - consideration of animal sex and provision of supportive care to advance model development. Int J Radiat Biol. 2021;97:126–130. [PubMed: 33259246]
64. Kiang JG, Cannon G, Olson MG, Smith JT, Anderson MN, Zhai M, et al. Female mice are more resistant to the mixed-field (67% Neutron + 33% Gamma) radiation-induced injury in bone marrow and small intestine than male mice due to sustained increases in G-CSF and the Bcl-2/Bax ratio and lower miR-34a and MAPK activation. Radiat Res. 2022;198:120–133. [PubMed: 35452510]

A

genotype	upregulated	downregulated	total
	irradiated		
WT	982	1241	2223
	44.1%	55.9%	
KO	1085	1378	2463
	44.0%	56.0%	
	basal		
KO vs. WT	69	16	85
	81.2%	18.8%	

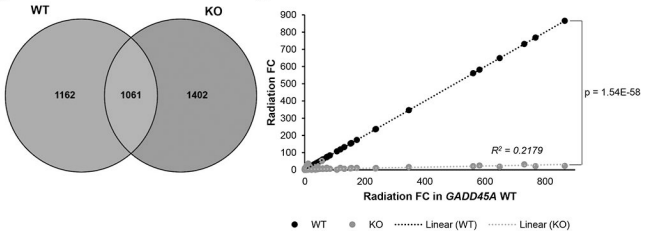

FIG. 1.

Differentially expressed genes. Panel A: Significantly differentially expressed genes in wild-type and GADD45A knockout (KO) mouse blood after 7 Gy X-rays relative to unirradiated mice and under basal conditions comparing the two genotypes. Total number and percentage of upregulated and downregulated of significantly differentially expressed genes in WT and KO mouse blood ($p < 0.001$) on day 1 following 7 Gy X-rays relative to unirradiated mice and under basal conditions comparing KO versus WT mice. Panel B: Venn diagram showing overlap of genes that are differentially expressed in response to 7 Gy X-rays. Panel C: Impact of GADD45A on the fold-change of radiation response signature genes. Fold changes (FC) in differentially expressed genes from irradiated mice of GADD45A KO mice compared with radiation fold changes (FC) of differentially expressed genes from irradiated wild-type mice. R2 values represent the fit of the gene fold changes to a line. P values were calculated using the paired Student's t-test. WT: wildtype; KO: *GADD45A* knockout.

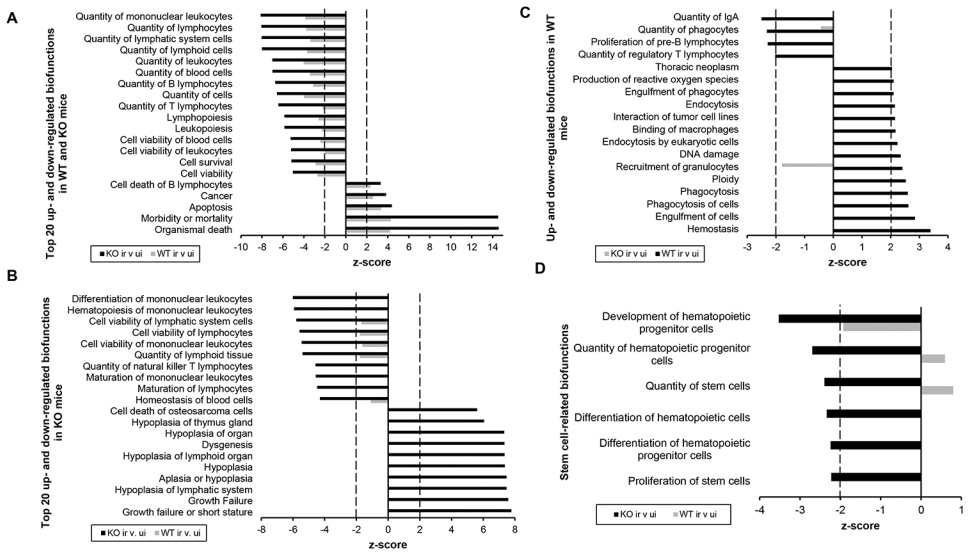

FIG. 2.

Diseases and functions significantly over- or under-represented in wild-type and *GADD45A* knockout mice identified by IPA. Panel A: Top 20 biofunctions commonly differentially regulated in both genotypes. Panel B: Top-20 functions overrepresented in wild-type irradiated mice. Panel C: Top-20 biofunctions overrepresented in GADD45A knockout mice. Panel D: Stem cell-related diseases and functions significantly over- or under-represented in wild-type and *GADD45A*-null. Functions displaying an absolute |z| score greater than 2.000 (marked by a dotted line) and showing Benjamini-corrected p value < 0.05 were considered significant. WT: wild-type; KO: GADD45A knockout; ir: irradiated; ui: unirradiated.

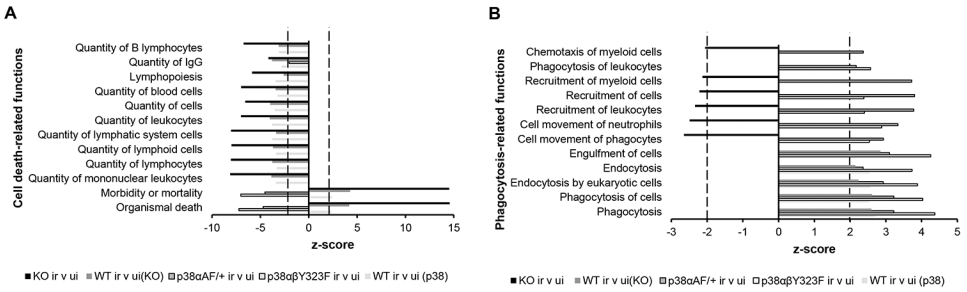

FIG. 3.

Death- (Panel A) and phagocytosis- (Panel B) related functions in wild-type, p38DKI, p38DN, and GADD45A KO mice exposed to 7 Gy X-rays. Functions displaying an absolute |z| score greater than 2.000 (marked by a dotted line) and showing Benjamini-corrected p value < 0.05 were considered significant. WT: wild-type; KO: GADD45A knockout; $p38\alpha\beta^{Y323F}$: p38 MAPK double knockin; $p38\alpha^{AF/+}$: p38MAPK dominant negative; ir: irradiated; ui: unirradiated.

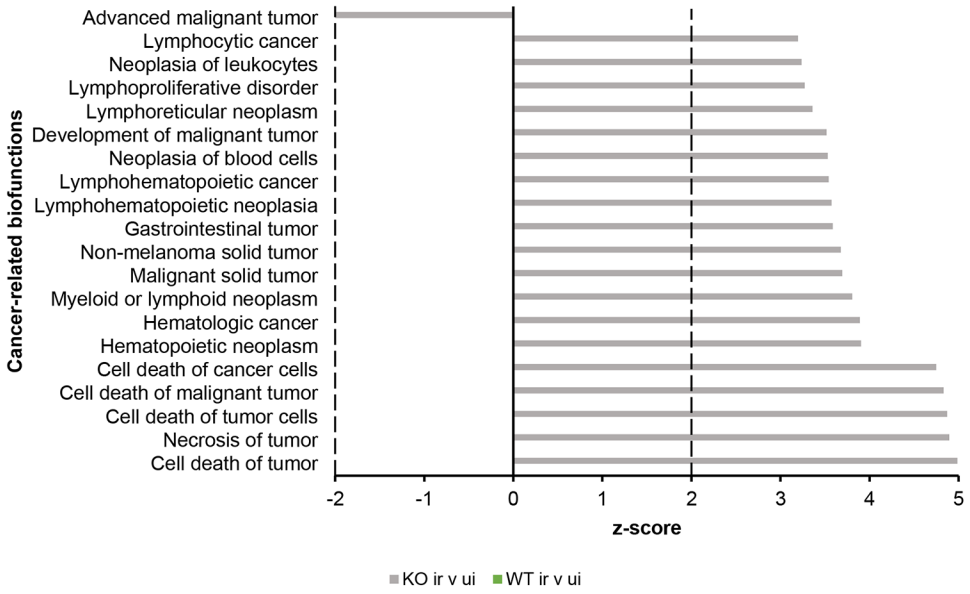

FIG. 4.

Cancer-related functions. Enriched cancer-related functions in irradiated wild-type and GADD45A knockout mouse blood compared with control (unirradiated) animals. A p value < 0.05 and an absolute |z| score 2.000 (marked by the dotted lines) were considered significant. WT: wild-type; KO: GADD45A knockout; ir: irradiated; ui: unirradiated.

TABLE 1

Top 10 upregulated and top 10 down-regulated dose-responsive genes in wild-type male data

Symbol	Correlation coefficient with dose	Bonferroni adjusted p-value
C1qa	0.998	1.15E-06
C1qc	0.997	5.31E-06
Gaml3	0.996	1.40E-05
Pltp	0.996	2.08E-05
Phlda3	0.995	2.94E-05
Sdc3	0.995	3.66E-05
Saa3	0.995	4.90E-05
Oas1a	0.995	5.07E-05
Cd5l	0.994	5.50E-05
Serpinb2	0.994	7.22E-05
Irf8	−0.994	5.29E-05
Ccr6	−0.995	2.95E-05
H2-Ob	−0.995	2.84E-05
H3.5	−0.995	2.60E-05
H2-Eb1	−0.996	2.14E-05
Serinc1	−0.996	2.02E-05
H2-Aa	−0.996	1.11E-05
H2-DMb1	−0.996	9.24E-06
H2-Ab1	−0.997	5.10E-06
Vpreb3	−0.998	1.45E-06

TABLE 2

Comparison of actual and reconstructed radiation doses

Genotype	*Actual Dose (Gy)*	*Reconstructed dose (Gy)*	
		Mean	**SD**
WT	0	0.00	0.03
	7	7.00	0.18
KO	0	0.30	1.64
	7	6.91	0.72
RMSE on testing data:		**1.05 Gy**	
MAE on testing data:		**0.85 Gy**	
R^2 on testing data:		**1.00**	

WT: wild-type; KO: GADD45A knockout; RMSE: Root Mean Square Error; MAE Mean of Absolute value of Errors.